Performance of High Resolution Chopper Spectrometer (HRC)

Shinichi Itoh[1], Tetsuya Yokoo, Daichi Kawana, Shin-ichiro Yano[*], Setsuo Satoh, Taku J. Sato[**], Takatsugu Masuda[**], Hideki Yoshizawa[**]

Institute of Materials Structure Science, High Energy Accelerator Research Organization, Tsukuba, 305-0801, Japan
[*]Graduate School of Science, Aoyama Gakuin University, Sagamihara, 252-5258, Japan
[**]The Institute for Solid State Physics, The University of Tokyo, Tokai, 319-1106, Japan

E-mail: shinichi.itoh@kek.jp

Abstract. To study condensed-matter dynamics over a wide energy-momentum space with high resolution, we constructed the High Resolution Chopper Spectrometer (HRC) at the beamline BL12 in the Materials and Life Science Experimental Facility (MLF) of the Japan Proton Accelerator Research Complex (J-PARC). With the construction nearly completed, we proceeded to characterize HRC. We confirmed that, under limited conditions, the neutron intensity and energy resolution of HRC agree well with the design values. We also installed the data acquisition (DAQ) system on HRC. In inelastic neutron scattering experiments with HRC, the event data of the detected neutrons are processed in the DAQ system and visualized in the form of the dynamical structure factor. We confirmed that the data analysis process works well by visualizing excitations in single-crystal magnetic systems. Moreover, the current status of HRC, including the earthquake damage, is reported.

1. Introduction

The High Resolution Chopper Spectrometer (HRC) was installed at BL12 in MLF, J-PARC [1,2]. HRC delivers high-resolution and relatively high-energy neutrons for a wide range of studies on the dynamics of materials, and three types of experiments can be considered for HRC, as indicated in Fig. 1. The first technique targets high-resolution experiments in a conventional energy momentum space (region A in Fig. 1). This experimental condition is useful for simultaneously determining a dispersion relation of excitations and details of the dynamical structure factor. The second technique aims to access the first Brillouin zone by using low-angle detectors and high-energy neutrons (region B). Observation of ferromagnetic spin waves from a polycrystalline sample becomes possible and should be useful for material development. The third technique opens the possibility of accessing eV region (region C). Dispersive excitations up to sub-eV region can be observed by using single-crystal samples. Electronic excitations are also expected to be observable if eV neutrons are utilized.

---

[1] To whom any correspondence should be addressed.

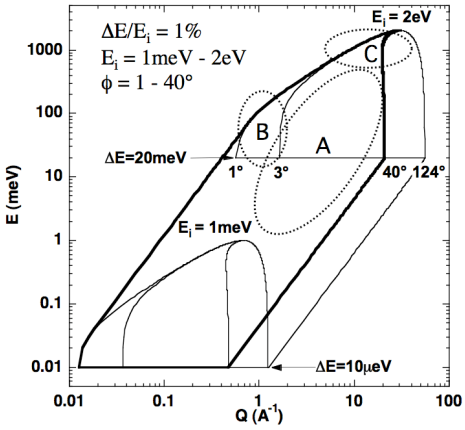

Fig. 1 Energy-momentum space for three techniques of high-resolution experiments A, B, and C proposed for HRC.

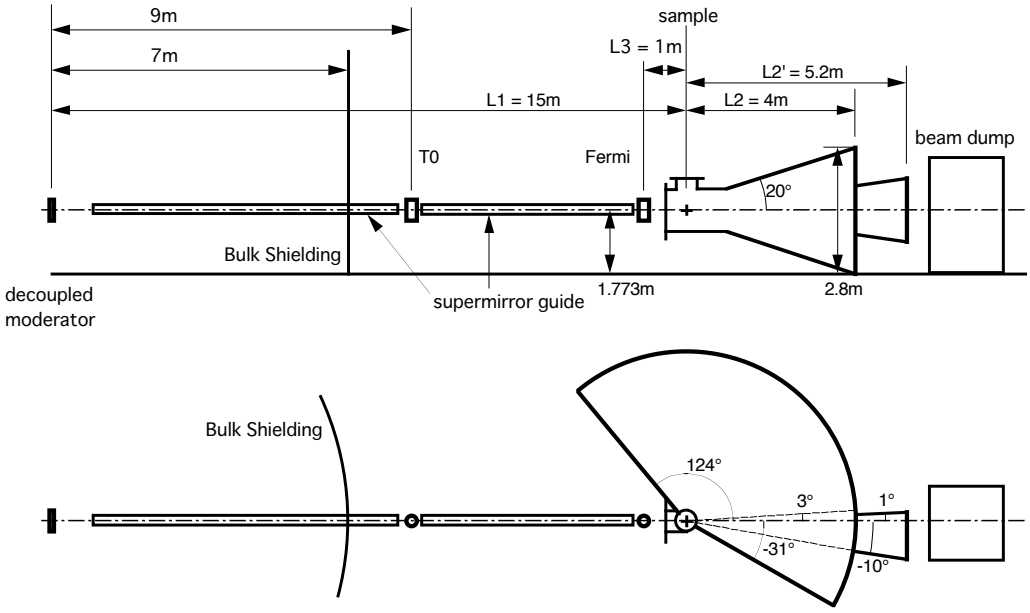

Fig. 2 Schematic layout of HRC.

2. Design and construction

A schematic layout of HRC is illustrated in Fig. 2. The size parameters are L_1 = 15 m (the distance between the neutron source and the sample), L_2 = 4 m (the distance between the sample and the detector), and L_3 = 1 m (the distance between the Fermi chopper and the sample). HRC at BL12 faces the decoupled moderator, which has an area of 100 mm × 100 mm, and the maximum sample size is assumed to be 50 mm × 50 mm. In this geometrical condition, the energy resolution is estimated to be $\Delta E/E_i$ = 2.5% (E_i: incident neutron energy) for the optimum condition where the chopper-open time Δt_{ch} is equal to the pulse width Δt_m, and the incident beam divergence is estimated to be $\Delta\phi$ = 5 mrad. The energy resolution can be improved when $\Delta t_{ch} < \Delta t_m$, with a concomitant reduction in the peak neutron intensity. For $\Delta E/E_i$ = 1%, the peak neutron intensity is 75% of that for the optimum condition, which we consider to be an acceptable tradeoff.

A Fermi chopper was installed at L_3 = 1 m. We developed the Fermi chopper by modifying a turbo molecular pump (TMP) with a magnetic bearing system [3]: the TMP blade was replaced by the slit

package, the TMP controller was used for controlling the magnetic bearing system, the motor of this system was driven by an external power supply, and the rotational phase was synchronized with the production timing of pulsed neutrons. Based on the developments, we produced a Fermi chopper. The commercially available composites made of boron fibers were used for the slit materials. In this actual system, we confirmed the phase control accuracy less than 0.1 μs (FWHM) at 600 Hz of the rotational frequency against the timing of the external trigger at an off-beam environment as well as the standard resolution (energy resolution for the optimum condition) of $\Delta E/E_i$ = 2.5 % in an on-beam experiment on the HRC. A shifting mechanism of two Fermi choppers was also developed in order to select one of the choppers (a standard resolution chopper and a high flux chopper) or white beam condition.

A T0 chopper, which we also developed [4], was installed at 9 m from the neutron source. At this position, the beam cross section was 76 mm × 76 mm. The size of the T0 chopper blade was chosen to be 78 mm × 78 mm, including a ±1 mm margin for the beam cross section, and the length of the blade along the beamline was 300 mm. The blade was made of Inconel X 750, which was chosen for its mechanical strength and radiation properties. When the blade center is initially centered on the beamline, it takes 408 μs for the blade to be removed from the beam cross section, and this occurs at a 100 Hz rotational frequency and for a 300 mm rotational radius. The rotational axis is parallel to and under the beamline. Under these conditions, HRC accepts neutrons with energy less than 2.5 eV. The margin of ±1 mm corresponds to a phase-control accuracy of ±5 μs at 100 Hz. We developed a phase control system which reduces the fluctuations in the rotational period down to 1 μs (FWHM) at 100 Hz at an off-beam environment. Also, the fluctuations during beam time were measured to be approximately 3 μs (FWHM) at any rotational frequency. The observed fluctuations meet the requirement demanded by the phase-control accuracy within ±5 μs. We successfully reduced the background noise at neutron energies near 0.5 eV by two orders of magnitude. Also, we confirmed that the transmission recovers below 2.5 eV of the neutron energy at 100 Hz, as designed. The energy for 50% transmission at 100 Hz is 10 eV, and then neutrons with energies up to several eV can be used with only a slight reduction in neutron intensities.

To increase the neutron flux, a supermirror guide tube was installed in the primary flight path in the shutter section (m = 3), in the biological shielding section (m = 3.65) and in the down stream section (m = 4), where m is the ratio of the critical wave number for the supermirror to that for natural nickel. The m values were dependent on by the financial budgets provided.

The vacuum scattering chamber encompasses the sample area and the detector system, and we installed position sensitive detectors (PSDs) for detecting scattered neutrons [1,2]. Although it was possible to install detectors from –31° to 124° in the scattering angle, the detectors covered only from –10° to 40° at present because of the recent limitations in He-3 gas supplies. Therefore, the installed detector area is only 30% of the entire area. In the main detector area from 3° to 40°, 128 pieces of PSDs (effective length: 2.8 m, diameter: 0.75”, He-3 gas pressure: 1.8 MPa) were mounted inside the vacuum chamber at L_2 = 4 m for conventional experiments. At low angles from –10° to 1°, 123 pieces of shorter PSDs (0.8 m, 0.5”, 2 MPa; 0.6 m, 0.5”, 2 MPa; 0.6 m, 1”, 1 MPa; used at KENS or newly acquired) were mounted outside the vacuum chamber: some at L_2 = 4 m and the rest at L_2 = 5.2 m at the lowest angles. These detectors are for experiments involving low-angle inelastic neutron scattering. These arrays of PSDs cover ±20° vertically. To install PSDs outside the vacuum chamber, a large area window was mounted on the chamber surface facing the detector system, and this window was made of a thin aluminum plate with 1.5 mm in thickness to reduce the loss of neutron intensities by scattering from the window material [5]. The inner surface of the vacuum chamber and the surface of vanes separating some scattering-angle regions (chamber volume: 50 m^3, surface: 175 m^2) were covered with B_4C resin to avoid neutron-scattering noise from the chamber material surface [6].

The data acquisition (DAQ) system for HRC is illustrated in Fig. 3 [2]. Signals generated at a PSD are amplified and sent to a readout module called NEUNET. When a neutron is captured at PSD n_{det}, the charges generated at both ends of the PSD are digitized and converted to digital pulse heights Q_1 and Q_2 by an analog-to-digital converter (ACD) in the NEUNET, where, in an ideal case, the position

of the detected neutron within the PSD is given by $u = L_D Q_2/(Q_1+Q_2)$ with the PSD length L_D. A timing signal from the accelerator control system defining $t = 0$ is delivered by a GATENET to NEUNETs and the time-of-flight of the detected neutron (t) is determined. The timing signal is gated by the device status, which is the phasing status of the Fermi chopper and the T0 chopper with respect to the timing, the temperature of the sample, etc. Thus, the GATENET does not forward the timing signal to the NEUNETs unless the device status indicates that all devices are operational. For detection of a neutron, the set $\{n_{det}, Q_1, Q_2, t\}$ is generated as an event datum (8 bytes/event) on the NEUNET. Event data can be accessed through a computer network with SiTCP, which is a high-speed transmission control protocol (TCP) processor. In addition, event data from the monitor detectors can be accessed at the GATENET through the computer network with SiTCP. One NEUNET controls 8 PSDs and 33 NEUNETs control 251 PDSs on HRC. The event data are transferred from the NEUNETs to the central processing unit (CPU). We installed the DAQ middleware on the CPU for the DAQ system (DAQ CPU). Via the DAQ Middleware, the DAQ-Operator configures the DAQ system and controls the processes in the DAQ system. User commands such as begin/end of the data acquisition can be sent to the DAQ system through a web-browser user interface.

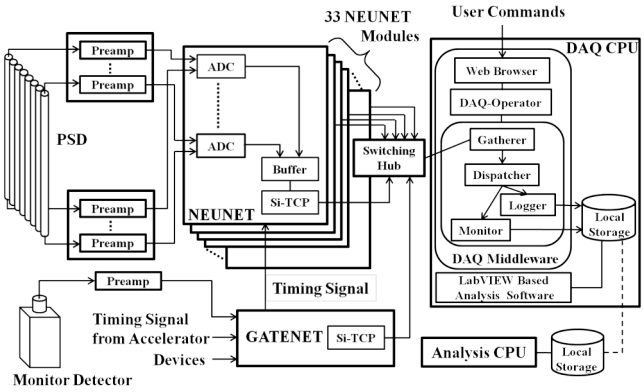

Fig. 3 DAQ system installed on HRC.

3. Performance

To evaluate the HRC performance, a vanadium standard sample was mounted at the sample position on HRC. A monochromatic neutron beam with the Fermi chopper or a white neutron beam without the Fermi chopper was incident on the sample, and the scattered neutrons were detected with the array of 128 pieces of PSDs located at scattering angles between 3° and 40°. A monitor detector was located at 13.4 m from the neutron source (just upstream of the Fermi chopper). The neutron intensities detected by the monitor and by the PSD array for the white beam are plotted in Figs. 4 (a) and 4 (b), respectively. The observed intensities were in good agreement with the calculations in the absolute values within a factor [1]. Figure 4 (c) shows the elastic scattering energy spectrum from the vanadium standard sample and detected by the PSD array for the incident neutron energy of $E_i = 206$ meV, with the standard resolution chopper (which provides roughly $\Delta t_{ch} = \Delta t_m$) with 600 Hz, as a function of the energy transfer [3]. We chose $E_i = 206$ meV, because the neutron transmission through the chopper shows a maximum at 200 meV with 600 Hz. The solid line is a calculated spectrum without any adjustable parameters. The energy resolution from the observed energy width was obtained to be $\Delta E = 5.4$ meV by a Gaussian fit to the observed spectrum, and therefore we confirmed $\Delta E/E_i = 2.5\%$ and the absolute neutron intensity in agreement with the calculation. It should be noted that during these measurements the supermirror section between the T0 chopper and the Fermi chopper was a collimator without supermirrors. Assuming the optimum condition ($\Delta E/E_i = 2.5\%$ with $\Delta t_{ch} = \Delta t_m$) for any E_i, the neutron flux for inelastic neutron scattering experiments at the sample position with a 1 MW proton beam for full installation of the guide tube is estimated as shown in Fig. 4 (d).

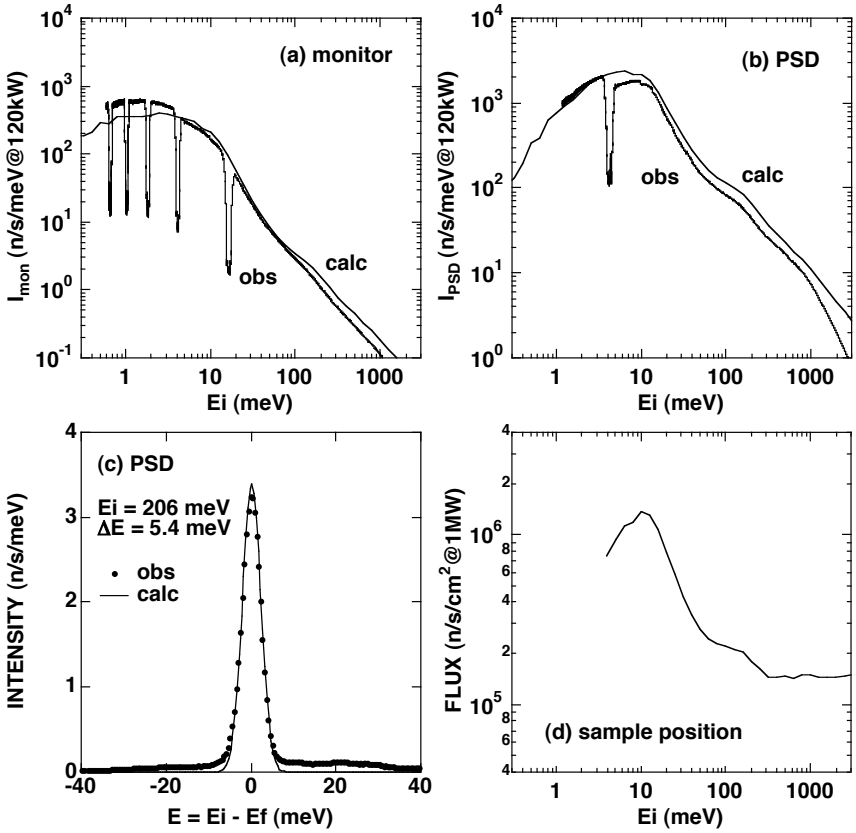

Fig. 4 Neutron intensities at the monitor (a) and at the PSD array (b) for white neutron beam. The dips in the observed data are caused by the operation of the T0 chopper. (c) Elastic-scattering energy spectrum at PSD array for vanadium standard sample with E_i = 206 meV. (d) Expected neutron flux at sample position for $\Delta E/E_i$ = 2.5% for 1 MW proton beam.

4. Observation of magnetic excitations

We measured magnetic excitations in the one-dimensional antiferromagnet $CsVCl_3$ at 20 K above the Néel temperature (T_N = 13.3 K), where the one-dimensional nature is dominant. It took 56 hours for the sample and 24 hours for the empty scan at 120 kW of proton-beam power. The intensity from the sample subtracted from the data for the empty scan is indicated in Fig. 5 (a) [2]. We clearly observed the dispersion curve of the antiferromagnetic excitations starting at the magnetic zone center around q ~ 1 Å^{-1}, the excitations near the magnetic zone boundary near q ~ 1.5 Å^{-1}, and E = 75 meV. This experiment indicates that the overall excitations can be clearly observed in 56 hours, which is expected to be reduced to only 7 hours when operating at full power (1 MW) at J-PARC. On HRC, the counting rate is greatly improved by using long PSDs, and the energy and the momentum resolutions are also improved by intensities integrated within a PSD after correcting the energy transfers at the positions of detected neutrons with high-positional-resolution PSDs. As the result, the dispersion curve including the weak-intensity parts was clearly observed. Also, inelastic neutron scattering experiments in a three-dimensional system MnP, which is a ferromagnetic intermetallic compound below T_C = 291 K, were performed. The dispersion relation of ferromagnetic magnons in the energy momentum space exhibits a parabolic surface whose apex is on the reciprocal lattice point. Scattering intensities are observed on the ring crossing between the scanning surface of the detectors and the parabolic dispersion surface. The ring centered at k = 2 rlu and E = 10 meV shown in Fig. 5 (b) is the magnon intensity around (020) [2]. Phonons also exist in the same position, so magnons could be separated from phonons by comparing the data at the paramagnetic state at 300 K. It should be noted that for these measurements the flight path between the T0 chopper and the Fermi chopper was a collimator without supermirrors.

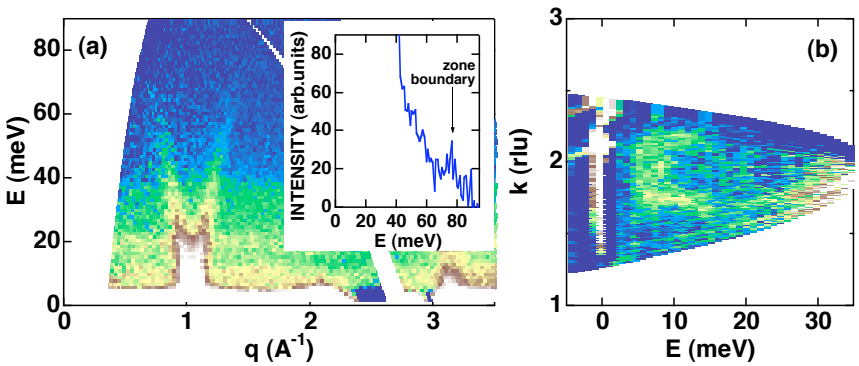

Fig. 5 Excitation spectrum in $CsVCl_3$ observed at 20 K with E_i = 100 meV on HRC (a). The inset shows the energy spectrum observed at a detector whose scan trajectory passes through the magnetic zone boundary. Excitation spectrum in MnP observed at 60 K with E_i = 35.8 meV on HRC indicating in (k,E) plane with l = 0 (b).

5. Further developments

The construction of HRC was nearly complete except for the coverage of the PSD array and we characterized its performance. We confirmed that, under limited conditions, the neutron intensity and the energy resolution were in good agreement with the design values. Also, we verified the data acquisition process and data analysis process by visualizing excitations in one- and three-dimensional single-crystal magnetic systems in inelastic neutron scattering experiments. At present, the optimum energy resolution of $\Delta E/E_i$ = 2.5 – 3 % is available for E_i = 10 – 500 meV.

Due to the earthquake disaster on 11 March 2011, some pieces of 2.8m PSDs were damaged and some shieldings were slipped on HRC. We realigned the beamline, restored the shieldings, replaced the damaged PSDs with new PSDs, and confirmed the operations of the choppers as well as the vacuum system. After these recovery works, the neutron production target at MLF received the proton beam in December 2011 and the neutron scattering experiments were started in January 2012.

During the recovery works, we improved the performance of HRC. The supermirror guide tube was fully installed, and then the neutron flux was increased by a factor of 3 at E_i = 100 meV and 5 at 50 meV. A Soller collimator system was installed just upstream of the sample, and the collimation can be chosen to be 2.3° and 0.6° automatically. Since there was a background noise at low angles previously, a measurement with an empty can was necessary to obtain such a spectrum as shown in Fig. 5. However, at present, a similar spectrum can be obtained by using the 2.3° collimator without an empty scan. In the low angle region, PSDs are installed down to 0.5°. Although there still exits large background noise around the lowest angle even by using the 0.6° collimator, we successfully observed spin wave excitations from the polycrystalline sample of the ferromagnet $La_{1.8}Sr_{0.2}MnO_3$ by a background correction.

[1] Itoh S, Yokoo T, Satoh S, Yano S, Kawana D, Suzuki J, Sato T J 2011 *Nucl. Instr. Meth. Phys. Res. A* **631** 90

[2] Yano S, Itoh S, Satoh S, Yokoo T, Kawana D, Sato T J 2011 *Nucl. Instr. Meth. Phys. Res. A* **654** 421

[3] Itoh S, Ueno K, Yokoo T 2012 *Nucl. Instr. Meth. Phys. Res. A* **661** 58

[4] Itoh S, Ueno K, Ohkubo R, Sagehashi H, Funahashi Y, Yokoo T 2012 *Nucl. Instr. Meth. Phys. Res. A* **661** 86; 2011 *ibid* **654** 527

[5] Itoh S, Yokoo T, Suzuki J, Teraoku T, Tsuchiya M 2012 *Nucl. Instr. Meth. Phys. Res. A* **670** 1

[6] Yokoo T, Kaneko N, Itoh S, Otomo T, Suzuya K, Suetsugu Y, Shirai M 2011 *Rev. Sci. Instrum.* **82** 095109